Sound Field Synthesis of Uniformly Moving Virtual Monopoles

GERGELY FIRTHA AND PETER FIALA
(firtha@hit.bme.hu) (fiala@hit.bme.hu)

Budapest University of Technology and Economics, Budapest, Hungary

Physical synthesis of the sound field that is generated by a moving virtual sound source has been the subject of extensive research in the recent decade. The article presents a new analytical modeling approach based on the wavenumber domain representation of the field emitted by a virtual monopole under uniform motion. Explicit and implicit frequency domain driving function expressions are derived for planar and linear secondary sources using the Spectral Division Method (SDM) and Wave Field Synthesis (WFS). The proposed method results in analytically correct driving functions and thereby correct synthesis of the Doppler effect.

1 INTRODUCTION

Sound Field Synthesis (SFS) aims at the physically correct synthesis of a virtual sound field by driving a set of secondary loudspeakers with appropriate driving signals. The objective of SFS is to provide proper driving functions to the secondary source distribution (SSD) so that the superposition of their individual sound fields results in the desired virtual sound field over a listening area.

When analytical SFS techniques are developed, the target sound field is most often a plane wave or the field induced by a virtual point source, whereas the loudspeaker arrangement is typically linear, planar, circular or spherical due to available analytic closed form expressions for driving functions. For the case of linear or planar SSD the most prominent technique is Wave Field Synthesis (WFS), based on the Rayleigh integral formulation of the virtual sound field [1–3]. For circular and spherical SSDs most techniques rely on Ambisonics, which gives an explicit formulation of the driving signals based on mode-matching in the spherical harmonic domain [4–7]. Besides the WFS, an Ambisonic-like mode-matching solution—termed the Spectral Division Method (SDM)—has been recently introduced [8, 6], which gives an explicit solution to the problem in the spectral (wavenumber) domain.

In addition to the SFS of stationary sources, the synthesis of moving sound sources has gained an increasing interest. A typical example is the synthesis of dynamic sound-scenes in virtual reality or cinema sound systems. In these applications, the proper reconstruction of the Doppler effect is of primary importance.

Early implementations of WFS with moving sources simulate the source motion as a sequence of stationary positions [9]. The technique results in a Doppler-like frequency variation, however, the generated sound field suffers from several artifacts. In conjunction with the deviation from the physically correct Doppler-frequency shift, a spectral broadening arises that makes the correct synthesis of an arbitrary wave front unfeasible. A recent approach attempts to incorporate the physical description of moving source dynamics into 3D WFS [10, 6]. The method provides mathematically correct time-domain driving functions for planar secondary sources. However, for a linear SSD a mathematically inconsistent solution was presented.

The present article revisits the SFS for virtual sound sources moving with a uniform speed. An analytical approach is formulated that reproduces the target sound field using a linear SSD. Analytical driving function expressions are presented both in the wavenumber domain using SDM and in the space-frequency domain by applying the established WFS approximations.

The article is structured as follows: Sec. 2 briefly reconsiders the main concepts of SDM and WFS. Sec. 3 derives the frequency and wavenumber domain representations of the field generated by a moving virtual monopole source. Sec. 4 applies the results of Sec. 3 for synthesis using both SDM and WFS. Finally, Sec. 5 presents numerical validation of the developed driving function expressions.

2 PRINCIPLES OF SOUND FIELD SYNTHESIS

The general arrangement used throughout this article is shown in Fig. 1. The listening area is the $[x, y > 0, 0]^{\mathrm{T}}$ half plane. The secondary sources are modeled as identical

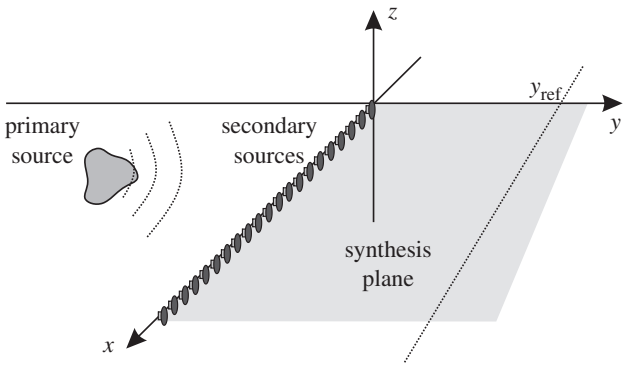

Fig. 1 SFS geometry under discussion.

point sources forming an infinite linear distribution along the x-axis.

If the SSD is driven by the driving function $D(x_0, \omega)$, where ω denotes the temporal angular frequency, then the frequency content $P(\mathbf{x}, \boldsymbol{\omega})$ of the synthesized sound field at the location $\mathbf{x} = [x,\ y,\ z]^{\mathrm{T}}$ is expressed as [6]

$$P(x, y, z, \boldsymbol{\omega}) = \int_{-\infty}^{\infty} D(x_0, \boldsymbol{\omega})\, G(x - x_0, y, z, \boldsymbol{\omega}) \mathrm{d}x_0, \quad (1)$$

where $G(\mathbf{x}, \boldsymbol{\omega})$ denotes the field of a secondary point source located at the origin. For 3D problems secondary source elements are most often modeled as acoustic monopoles, where $G(\mathbf{x}, \boldsymbol{\omega}) = \mathrm{e}^{-\mathrm{j}k|\mathbf{x}|}/4\pi|\mathbf{x}|$ is the 3D full space, freefield Green's function, and $k = \frac{\omega}{c}$ is the acoustic wavenumber. The derived linear driving function is often referred as 2.5D driving function, referring to the fact that instead of the 2D Green's function 3D point sources are used for 2D SFS problem as well [1].

2.1 Spectral Division Method

The explicit solution for the reproduction problem relies on the fact that integral Eq. (1) represents a convolution along the secondary source line. A temporal Fourier transform w.r.t. t and a spatial Fourier transform w.r.t. x yields the wavenumber domain representation $\tilde{P}(k_x, y, z, \boldsymbol{\omega})$ of the synthesized field in the form of a spectral product. Specifically, the desired field on the reference line can be formulated as

$$\tilde{P}(k_x, y_{\mathrm{ref}}, 0, \boldsymbol{\omega}) = \tilde{D}(k_x, \boldsymbol{\omega})\, \tilde{G}(k_x, y_{\mathrm{ref}}, 0, \boldsymbol{\omega}), \quad (2)$$

and the driving function is computed by a spectral division:

$$\tilde{D}(k_x, \boldsymbol{\omega}) = \frac{\tilde{P}(k_x, y_{\mathrm{ref}}, 0, \boldsymbol{\omega})}{\tilde{G}(k_x, y_{\mathrm{ref}}, 0, \boldsymbol{\omega})}. \quad (3)$$

The SDM employs no approximation, ensures perfect synthesis on the reference line, and can be therefore regarded as a reference solution. However, direct applications require the inverse spatio-temporal transform of the driving function $\tilde{D}$, which often cannot be calculated analytically.

2.2 Wave Field Synthesis

As the alternative of SDM, traditional WFS provides an implicit solution for the problem based on the Rayleigh-integral formulation of the virtual sound field. The Rayleigh integral represents the wave field in the half space $y > 0$ merely using boundary conditions on the boundary plane $y = 0$ [3]:

$$P(\mathbf{x}, \boldsymbol{\omega}) = \iint_{-\infty}^{\infty} \underbrace{-2\, \frac{\partial P(x_0, y, z_0, \boldsymbol{\omega})}{\partial y}\bigg|_{y=0}}_{D_{3\mathrm{D}}(x_0, z_0, \boldsymbol{\omega})} G(x - x_0, y, z - z_0, \boldsymbol{\omega}) \mathrm{d}x_0 \mathrm{d}z_0. \quad (4)$$

The Rayleigh integral provides a straightforward way of perfect SFS by driving a planar secondary monopole distribution with the normal derivative of the desired field at $y = 0$. In order to obtain the driving functions $D(x_0, \omega)$ for a linear secondary array, the stationary phase method [11] can be applied. The method is based on the second order Taylor series expansion of rapidly oscillating functions, followed by an analytical integration along the z-axis, and results in a frequency-dependent correction term [12, 3, 13]. As the result of the approximation, phase-correct synthesis is restricted to the *synthesis plane*, i.e., the horizontal plane containing the virtual sound source and the SSD. Furthermore, correct synthesis w.r.t. amplitude and phase is restricted to the *reference line*, parallel to the secondary sources. While for a planar SSD geometry SDM and WFS provide exactly the same result [14], linear WFS can be regarded as the far-field/high-frequency approximation of the linear SDM, as shown, e.g., in [13].

3 DESCRIPTION OF MOVING SOUND SOURCES IN THE SPECTRAL DOMAIN

The presented two approaches of SFS may be applied to arbitrary virtual sound fields, including the field of moving virtual sources. Application of WFS requires the normal derivative of the desired field on the boundary plane, SDM utilizes the wavenumber domain representation of the virtual field on the reference line. This section provides analytical expressions for the frequency and wavenumber content for a virtual spherical monopole source moving in an arbitrary direction along a infinite straight line in the $z = 0$ plane. First the case of the motion, parallel to the x-axis is introduced which is then extended in Sec. 3.2 for arbitrary inclination angles. The presented description can be applied for sources moving at subsonic velocities (i.e., $v < c$). As it was pointed out in [6], the SFS of sources moving at supersonic velocities is of little practical use as the human auditory system is not aware of the properties of the sound field generated by such a moving source.

3.1 Temporal Fourier Transform Representation

The description of the time history of the sound field generated by the moving source is analogous to that given in [6]. Consider a translation invariant, harmonically oscillating moving source located at $\mathbf{x}_s(\tau) = [x_s + v\tau,\ y_s,\ z_s]^{\mathrm{T}}$ and radiating with a source time history $q(\tau) = \mathrm{e}^{\mathrm{j}\omega_0\tau}$. The arrangement is depicted in Fig. 2. The sound field can be expressed as the response of a linear time-variant system

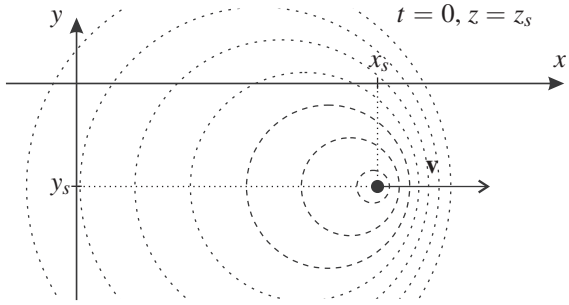

Fig. 2 Arrangement for description of a moving sound source.

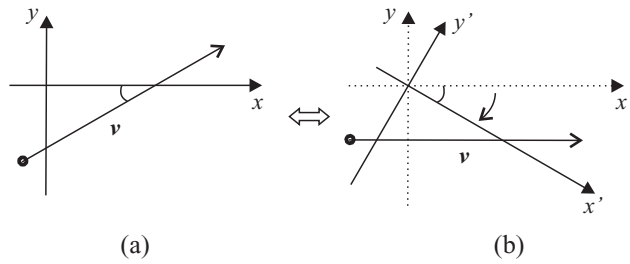

Fig. 3 The field of a source moving in arbitrary direction can be derived from a source, moving parallel with x-axis in a rotated coordinate system.

with a time-varying impulse response $g_{\mathrm{m}}(\mathrm{x}-\mathrm{x_s}(\tau),\tau)$:

$$p_{\mathrm{m}}(\mathbf{x},t)=\int_{(\tau)} g_{\mathrm{m}}(x-x_s-v\tau,\, y-y_s,\, z-z_s,\, t-\tau)\,\mathrm{e}^{\mathrm{j}\boldsymbol{\omega}_0\tau}\,\mathrm{d}\tau. \tag{5}$$

Expressing the source impulse response $g_{\mathrm{m}}(x, y, z, t)$ with the double inverse Fourier transform of its wavenumber-frequency domain representation $\tilde{G}_{\mathrm{m}}(k_x, y, z, \boldsymbol{\omega})$ results in

$$g_{\mathrm{m}}(x-x_s-v\tau, y, z, t-\tau)=\frac{1}{(2\pi)^2}\int_{(\boldsymbol{\omega}')}\int_{(k_x)}\tilde{G}_{\mathrm{m}}(k_x, y, z, \boldsymbol{\omega}')\,\mathrm{e}^{-\mathrm{j}k_x(x-x_s-v\tau)}\,\mathrm{d}k_x\mathrm{e}^{\mathrm{j}(t-\tau)\boldsymbol{\omega}'}\,\mathrm{d}\boldsymbol{\omega}'. \tag{6}$$

Performing a forward Fourier transform with respect to time, the frequency content P_{m} of the field of the moving virtual source is obtained as:

$$\begin{aligned}P_{\mathrm{m}}(\mathbf{x},\boldsymbol{\omega})&=\mathcal{F}_t\{p(x,y,z,t)\}\\&=\int_{(t)}\int_{(\tau)}\int_{(\boldsymbol{\omega}')}\int_{(k_x)}\frac{1}{4\pi^2}\,\tilde{G}_{\mathrm{m}}(k_x, y-y_s, z-z_s, \boldsymbol{\omega}')\\&\quad\mathrm{e}^{-\mathrm{j}k_x(x-x_s-v\tau)}\,\mathrm{d}k_x\,\mathrm{e}^{\mathrm{j}\boldsymbol{\omega}'(t-\tau)}\,\mathrm{d}\boldsymbol{\omega}'\,\mathrm{e}^{\mathrm{j}\boldsymbol{\omega}_0\tau}\,\mathrm{d}\tau\,\mathrm{e}^{-\mathrm{j}\boldsymbol{\omega}t}\mathrm{d}t.\end{aligned} \tag{7}$$

Reversing the order of integration, simplifying the Fourier transform of exponentials with Dirac delta functions and exploiting the sifting property of the Dirac delta function along with applying the similarity theorem, the following final expression for the frequency content is obtained:

$$P_{\mathrm{m}}(\mathbf{x},\boldsymbol{\omega})=\frac{1}{v}\,\tilde{G}_{\mathrm{m}}\left(\hat{k}, y-y_s, z-z_s, \boldsymbol{\omega}\right)\,\mathrm{e}^{-\mathrm{j}\hat{k}(x-x_s)}, \tag{8}$$

where $\hat{k}=\frac{\boldsymbol{\omega}-\boldsymbol{\omega}_0}{v}$.

For the case of a virtual monopole sound source, the wavenumber content $\tilde{G}_{\mathrm{m}}$ is written as

$$\tilde{G}_{\mathrm{m}}(k_x, y, z, \boldsymbol{\omega})=-\frac{\mathrm{j}}{4}H_0^{(2)}\left(-\mathrm{j}\,k_{\mathrm{t}}\,r_{\mathrm{t}}\right), \tag{9}$$

where $H_0^{(2)}$ denotes the Hankel function of the second kind and order 0, $r_{\mathrm{t}}=\sqrt{y^2+z^2}$ is the transversal distance, and $k_{\mathrm{t}}=\sqrt{k_x^2-(\boldsymbol{\omega}/c)^2}$ is the transversal wavenumber.

3.2 Sources Moving Inclined to the *x*-axis

The field of a virtual moving source arriving at the x-axis under a given angle of inclination φ can be formulated by a rotation of coordinate axes (refer to Fig. 3). The new coordinate system $\mathbf{x}'=[x', y', z]$ is defined by the relation

$$\begin{bmatrix}x' & y'\end{bmatrix}=\begin{bmatrix}\cos\varphi & \sin\varphi\\ -\sin\varphi & \cos\varphi\end{bmatrix}\begin{bmatrix}x-x_{\mathrm{s}} & y-y_{\mathrm{s}}\end{bmatrix}. \tag{10}$$

In the shifted and rotated coordinate system the source is located in the origin at the time origin and travels parallel to the x'-axis. According to Eqs. (8) and (9), for a moving monopole arriving at the x-axis at an angle φ, located at $t=0$ at $[x_{\mathrm{s}}, y_{\mathrm{s}}, 0]^{\mathrm{T}}$ the frequency content of the generated field is given by

$$P_{\mathrm{m}}(\mathbf{x},\boldsymbol{\omega})=-\frac{\mathrm{j}}{4v}\,H_0^{(2)}\left(-\mathrm{j}\,\hat{k}_t\,\sqrt{y'^2+z^2}\right)\,\mathrm{e}^{-\mathrm{j}\hat{k}x'}, \tag{11}$$

where $\hat{k}_t=\sqrt{\hat{k}^2-\left(\frac{\boldsymbol{\omega}}{c}\right)^2}$.

The same transform may be applied to the spatio-temporal description of a moving source, as given by [15, (11.2.13)] in order to describe the time history of a source moving at arbitrary direction in the original coordinate system:

$$p_{\mathrm{m}}(\mathbf{x},t)=\frac{1}{4\pi}\,\frac{\mathrm{e}^{\mathrm{j}\,\boldsymbol{\omega}_0\left(t-\frac{M(x'-v\,t)+\sqrt{(x'-v\,t)^2+(y'^2+z^2)(1-M^2)}}{c(1-M^2)}\right)}}{\sqrt{(x'-v\,t)^2+(y'^2+z^2)(1-M^2)}}, \tag{12}$$

with $M=\frac{v}{c}$ denoting the Mach number. In the following chapters this formulation will serve as a reference solution for numerical simulations.

3.3 Spatio-Temporal Fourier Transform Representation

The spatial Fourier transform of Eq. (11) is considered in the most relevant $z=0$ plane only. The wavenumber content can be given as (see the appendix for the derivation)

$$\tilde{P}_{\mathrm{m}}(k_x, y, 0, \boldsymbol{\omega})=\frac{\pi}{v|\sin\varphi|}\,\frac{\exp\left(-\mathrm{j}\,\hat{k}\,\frac{y-y_s}{\sin\varphi}\right)}{\sqrt{\left(\frac{\cos\varphi\,\hat{k}-k_x}{\sin\varphi}\right)^2+\hat{k}_t^2}}\,\exp\left(\mathrm{j}\,k_x\,\frac{\sin\varphi\,x_s+\cos\varphi\,(y-y_s)}{\sin\varphi}\right). \tag{13}$$

As the derivation utilizes the Fourier similarity theorem (see .2 in the Appendix), which is defined only for not-zero scaling ratio, the above expression is undefined for $\varphi=0$. However, the parallel case is easily handled by the direct transform of Eq. (8) where only the exponential

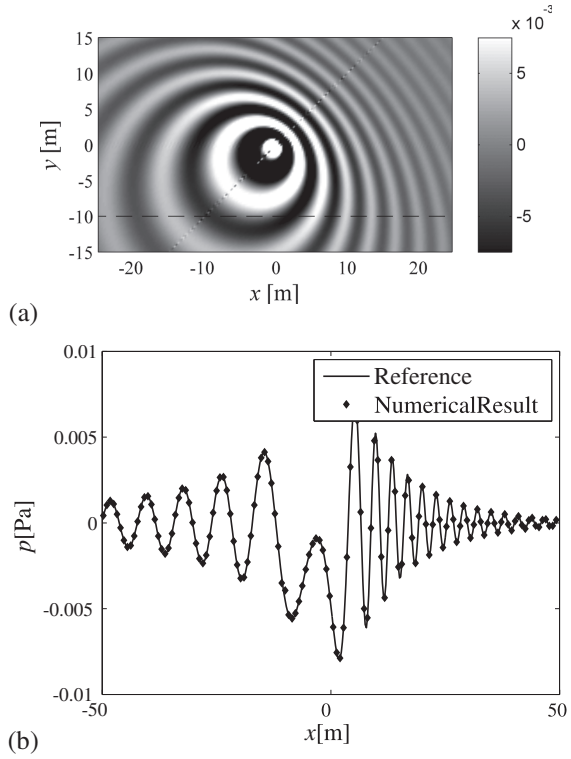

Fig. 4 (a) Snapshot of $\Re\{p_{\mathrm{m}}(\mathbf{x}, t)\}$ calculated in the wavenumber-frequency domain via double inverse transforming Eq. (13) and (b) the field compared with the reference solution (Eq. (12)) taken at $y = -10$ m.

term depends on x:

$$\tilde{P}_{\mathrm{par}}(k_x, y, 0, \boldsymbol{\omega}) = -\frac{\mathrm{j}}{4v} H_0^{(2)}\left(-\mathrm{j}\,\hat{k}_t\,|y - y_s|\right) \mathrm{e}^{\mathrm{j}\hat{k}\,x_s}\, 2\pi\delta(k_x - \hat{k}). \quad (14)$$

It can be proven, that Eq. (13) converges weakly into Eq. (14). The spectral representation of the field evoked by a moving virtual sound source is of primary importance in the aspect of SFS utilizing the SDM.

In order to demonstrate the applicability of the theoretical results, the sound field of a moving harmonic monopole is computed by means of the direct numerical evaluation of Eq. (13), followed by a double inverse Fourier transform. The point source travels with an angle of $\varphi = 45^\circ$, at a velocity of $v = 200$m/s, and radiates at $\omega_0 = 2\pi \cdot 60$rad/s. The results are depicted in Fig. 4. The perfect match with the reference solution Eq. (12) indicates the validity of both the derived frequency domain and wavenumber domain representations Eqs. (11)–(13).

4 SYNTHESIS OF MOVING SOUND SOURCES

4.1 2.5D Driving Functions for SDM

Having found the wavenumber domain representation of the virtual sound field, the application of the SDM for sound field synthesis is straightforward. The driving function is computed by a spectral division, cf., Eq. (3)

$$\tilde{D}(k_x, \boldsymbol{\omega}) = \frac{\tilde{P}_{\mathrm{m}}(k_x, y_{\mathrm{ref}}, 0, \boldsymbol{\omega})}{\tilde{G}(k_x, y_{\mathrm{ref}}, 0, \boldsymbol{\omega})}, \quad (15)$$

where $\tilde{P}$ is defined by Eq. (13) and $\tilde{G}$ is given by Eq. (9). For this general case only the wavenumber representation of the driving function is available. For a virtual source moving parallel to the secondary sources, using Eq. (14) the driving function simplifies to

$$\tilde{D}(k_x, \boldsymbol{\omega}) = \frac{2\pi}{v} \frac{H_0^{(2)}\left(-\mathrm{j}\,\hat{k}_t\,|y_{\mathrm{ref}} - y_s|\right)}{H_0^{(2)}\left(-\mathrm{j}\,k_t\,|y_{\mathrm{ref}}|\right)} \mathrm{e}^{\mathrm{j}\hat{k}\,x_s}\, \delta(k_x - \hat{k}). \quad (16)$$

The frequency domain representation of the driving function is obtained by means of an inverse Fourier transform. The sifting property of the Dirac-delta function can be exploited ($k_x = \hat{k}$). As $k_t|_{k_x=\hat{k}} = \hat{k}_t$, the resulting driving function is given by

$$D(x_0, \boldsymbol{\omega}) = \frac{1}{v} \frac{H_0^{(2)}\left(-\mathrm{j}\,\hat{k}_t\,|y_{\mathrm{ref}} - y_s|\right)}{H_0^{(2)}\left(-\mathrm{j}\,\hat{k}_t\,|y_{\mathrm{ref}}|\right)} \mathrm{e}^{-\mathrm{j}\hat{k}\,(x_0 - x_s)}. \quad (17)$$

This means that for the special case of a source, moving parallel to the SSD the spatial inverse transform can be carried out and an analytic closed reference solution was found.

4.2 3D and 2.5D Driving Functions for WFS

For the application of WFS with a planar SSD, the y directional derivative of the virtual sound field Eq. (11) needs to be formulated on the boundary plane $y = 0$ (cf., Eq. (4)). The resulting driving function is given as:

$$D_{3\mathrm{D}}(x_0, z_0, \boldsymbol{\omega}) = \frac{\mathrm{e}^{-\mathrm{j}\hat{k}\,x'}}{2v}\Big(\hat{k}\sin\varphi\, H_0^{(2)}(-\mathrm{j}\,\hat{k}_t\,r_t') - \frac{\hat{k}_t\cos\varphi\, y'}{r_t'} H_1^{(2)}(-\mathrm{j}\,\hat{k}_t\,r_t')\Big), \quad (18)$$

where $x' = \cos\varphi\,(x_0 - x_s) - \sin\varphi\, y_s$ and $y' = -\sin\varphi\,(x_0 - x_s) - \cos\varphi\, y_s$ with $r_t' = \sqrt{y'^2 + z^2}$. This driving function ensures perfect reconstruction in the $y > 0$ half-space.

In order to obtain the WFS driving functions for a linear SSD, the integration along the vertical direction in the Rayleigh integral needs to be carried out analytically. This can be done using the large-argument exponential approximation of the Hankel functions as given by [16, (10.2.5-6)], and applying the method of stationary phase for a fixed evaluation position $\mathbf{x}_{\mathrm{e}}$ at $z_0 = 0$ [12]. The obtained driving function reads

$$D(x_0, \boldsymbol{\omega}) = \frac{1}{v}\sqrt{\frac{r}{k\,|y'| - \mathrm{j}\,\hat{k}_t\,r}} \left(\sqrt{\frac{\hat{k}_t}{\mathrm{j}}}\cos\varphi + \sqrt{\frac{\mathrm{j}}{\hat{k}_t}}\,\hat{k}\sin\varphi\right) \mathrm{e}^{-\hat{k}_t\,|y'| - \mathrm{j}\hat{k}\,x'}, \quad (19)$$

where $r = |\mathbf{x}_{\mathrm{e}} - \mathbf{x}_0|$, with $\mathbf{x}_0 = [x_0, 0, 0]^{\mathrm{T}}$. This driving function is valid for a fixed observer position $\mathbf{x}_{\mathrm{e}}$. The

convolution expression for the synthesized field reads

$$P(\mathbf{x}_\mathrm{e}, \boldsymbol{\omega}) = \left(\sqrt{\frac{\hat{k}_t}{\mathrm{j}}}\cos\varphi + \sqrt{\frac{\mathrm{j}}{\hat{k}_t}}\,\hat{k}\sin\varphi\right)\frac{1}{v} \int_{-\infty}^{\infty}\sqrt{\frac{r}{k\,|y'| - \mathrm{j}\,\hat{k}_t\,r}}\,\frac{1}{4\pi\,r}\,\mathrm{e}^{-\hat{k}_t\,|y'| - \mathrm{j}(\hat{k}\,x' + k\,r)}\,\mathrm{d}x_0. \quad (20)$$

In order to achieve perfect synthesis along a reference line instead of a reference point, the same procedure is carried out as given in [1, Ch. 3.1] for stationary virtual sources. We suggest that the pressure in the evaluation point $\mathbf{x}_\mathrm{e} = [x_\mathrm{e}, y_\mathrm{ref}, 0]^\mathrm{T}$ is dominated by the contribution of one secondary source at $\mathbf{x}_0^* = [x_0^*, 0, 0]^\mathrm{T}$ and its close neighborhood. The secondary position $\mathbf{x}_0^*$ is obtained by finding the stationary point along the x-axis, where the derivative of the exponential in Eq. (20) with respect to x is zero. The resulting stationary distance $r_0 = |\mathbf{x}_\mathrm{e} - \mathbf{x}_0^*|$ is independent of the observation position, and can be expressed as

$$r_0 = |y_\mathrm{ref}|\sqrt{\frac{k^2}{(\hat{k}\sin\varphi - \mathrm{j}\,\hat{k}_t\cos\varphi)^2}}. \quad (21)$$

This wavenumber-dependent distance, substituted in place of r in Eq. (19) ensures amplitude correct synthesis on the reference line $y = y_\mathrm{ref}$.

$$D_\mathrm{2.5D}(x_0, \boldsymbol{\omega}) = \frac{1}{v}\sqrt{\frac{|y_\mathrm{ref}|}{(\cos\varphi + \mathrm{j}\,\frac{\hat{k}}{\hat{k}_t}\sin\varphi)\,|y'| + |y_\mathrm{ref}|}} \left(\cos\varphi + \mathrm{j}\,\frac{\hat{k}}{\hat{k}_t}\sin\varphi\right)\mathrm{e}^{-\hat{k}_t\,|y'| - \mathrm{j}\,\hat{k}\,x'}. \quad (22)$$

All three approximations are valid in the far-field, meaning that the synthesis will be correct only relatively far from the SSD.

For sources moving parallel to the SSD the driving function simplifies to

$$D_\mathrm{2.5D}(x_0, \boldsymbol{\omega}) = \frac{1}{v}\sqrt{\frac{|y_\mathrm{ref}|}{|y_s| + |y_\mathrm{ref}|}}\,\mathrm{e}^{-\hat{k}_t\,|y_s| - \mathrm{j}\,\hat{k}\,(x_0 - x_s)}. \quad (23)$$

It can be easily proven that the large argument approximation of the SDM solution given by Eq. (17) coincides with Eq. (23), meaning that similarly to the case for a stationary source, the two techniques lead to the same result in the far field.

A recent approach for WFS of a moving source obtains valid driving functions for planar secondary sources by evaluating the directional gradient of the description for a moving source in the time domain [6]. For linear secondary sources, however, it applies the constant correction term obtained for a stationary virtual source, and omits the spatio-temporal dependency of the angular frequency, measured along the SSD. As the derived driving function Eq. (22) is frequency-dependent, it is obvious that 2.5D correction will depend both on space and time. Therefore, the heuristic assumption about the prefiltering will lead to amplitude errors over the listening area—even on the reference line—as it was confirmed by simulations.

It is important to note that sources moving inclined to the x-axis will always be located in front of the SSD for a certain time interval. As it is a standard prerequisite for both SDM and WFS (not involving focusing), that the virtual source is located behind the SSD, the derived driving functions require special interpretation. From symmetry properties of the Rayleigh integral, the synthesized fields can always be interpreted as that of a moving source that bounces back from the the SSD with opposite amplitude and angle of reflection $\pi - \varphi$. Also, at the time instant when the virtual source reaches the SSD or the reference line, the driving function becomes singular, which is a direct consequence of the acoustic monopole's non-physical nature. Due to the mentioned two artifacts, the practical applications of the presented methods are restricted to space-time regimes when the moving source does not enter the listening area.

5 NUMERICAL EXAMPLES AND COMPARISON

5.1 Parallel Case

The first presented example is SFS of a harmonic monopole moving parallel to the secondary sources. The source is located at $\mathbf{x}_s = [0,\ -1,\ 0]^\mathrm{T}$ at the time origin and travels with a speed of $v = 200$m/s. The source frequency is $\omega_0 = 2\pi \cdot 50$rad/s. The secondary sources are located along the x-axis, and the reference line is at a distance of $y_\mathrm{ref} = 3$m from the secondary sources.

WFS simulation was carried out in the time domain, and the driving functions were obtained by performing the numerical inverse Fourier transform of Eq. (23). The length of the secondary source array was $L = 200$m, with a spatial resolution of $\Delta x = 0.2$m. The duration of the calculated pass-by was $T = 5$s, with a sampling frequency of $f_s = 8$kHz.

Fig. 5(a) displays the time history of the synthesized sound field at the observation point $\mathbf{x} = [0,\ y_\mathrm{ref},\ 0]^\mathrm{T}$ and compares the result of WFS with the analytical time domain reference solution given by Eq. (12). Apparently, the derived driving functions provide perfect reconstruction sufficiently far from the SSD.

Fig. 5(b) displays the instantaneous frequency of the synthesized signal as the function of time and compares the numerical results to the theoretical time-dependence of the observed frequency [15, (11.2.16)]. The perfect match between the theoretical and the synthesized results indicates the proper reproduction of the Doppler effect in time domain.

5.2 Inclined Case

The next numerical example is SFS of a monopole traveling in an inclined direction of $\varphi = 30^\circ$ with a velocity of $v = 200$m/s and oscillating at a source frequency $\omega_0 = 2\pi \cdot 20$rad/s. The source is located in the time origin at $\mathbf{x}_s = [0, -5, 0]^\mathrm{T}$ and the reference line is set to $y_\mathrm{ref} = 10$m. Again, the length of the SSD was 200 m, with a resolution of 0.25 m. In case of the planar synthesis the vertical length of the secondary plane was 100 m. The pass-by, with a duration of 5 s was sampled at $f_s = 1500$ Hz.

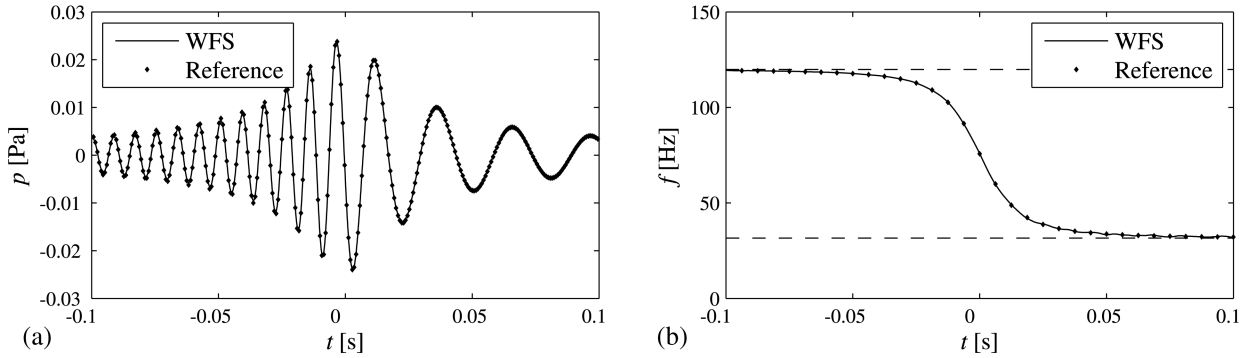

Fig. 5 (a) Time history and (b) measured instantaneous frequency of a virtual source pass-by using WFS.

For this setup, both WFS and SDM results are presented. The WFS provides analytical driving functions in the spatial-frequency domain, but the driving functions of the SDM are only available in the wavenumber domain. The numerical inverse Fourier transform of Eq. (15) may lead to several undesired effects as explained in the following.

Sampling in the k_x wavenumber domain results in aliasing in space, i.e., multiple virtual sources passing by in the same direction. To overcome aliasing, the spectrum of the driving function was oversampled by a factor of 3 and the space domain driving functions were low-pass filtered and decimated to achieve the final spatial resolution. The second numerical problem stems from the spectral division. As the spectrum of the stationary monopole decreases exponentially with the wavenumber k_x in the evanescent domain, the division may lead to large numerical errors. This is a well-known issue in the field of Near Field Acoustic Holography. To avoid round off errors, numerical regularization [11] is needed. The applied regularization method is low-pass filtering with a smooth transition at $k_x = \frac{\omega}{c}$.

Fig. 6 displays the snapshot of the analytically available target wave field and the result of the linear WFS at $t = 0$. It can be seen, that using the derived WFS driving functions phase correct synthesis of the original wave front can be achieved in the plane of synthesis. Amplitude deviations from the reference field are emphasized by plotting cross-sections of the synthesized fields: Fig. 7 compares the results of three SFS techniques by displaying the simulated field at $t = 0$ along the reference line. The techniques are (a) WFS with a planar SSD Eq. (18), depicted together with WFS with a linear SSD Eq. (22), and (b) SDM Eq. (15). The simulation results of all techniques are compared to the analytical solution.

As expected, the result of planar WFS provides perfect match. We note here that in this case the analytical virtual field is captured at any point in front of the secondary plane.

For the case of the linear WFS and the SDM slight amplitude errors occur. Linear WFS yields the largest deviations around the location $x = 0$. These errors are caused by the horizontal stationary phase approximation applied in Eq. (22).

Although the SDM should ensure a perfect synthesis on the reference line, Fig. 7(c) shows growing amplitude errors with increasing x. These errors originate from the spatial aliasing and can be reduced by higher oversampling of the wavenumber spectrum. Besides the amplitude errors both techniques applying linear secondary arrays result in a phase-correct synthesis on the reference line. This confirms the validity of the theoretical results given in the previous sections.

6 CONCLUSION

This article presented an analytical approach for the description and synthesis of moving virtual sound sources.

Based on the spectral description of a moving source, an analytical expression was formulated for the frequency and wavenumber content of a virtual monopole traveling in an arbitrary horizontal direction. By utilizing the spectral description and applying the method of stationary phase,

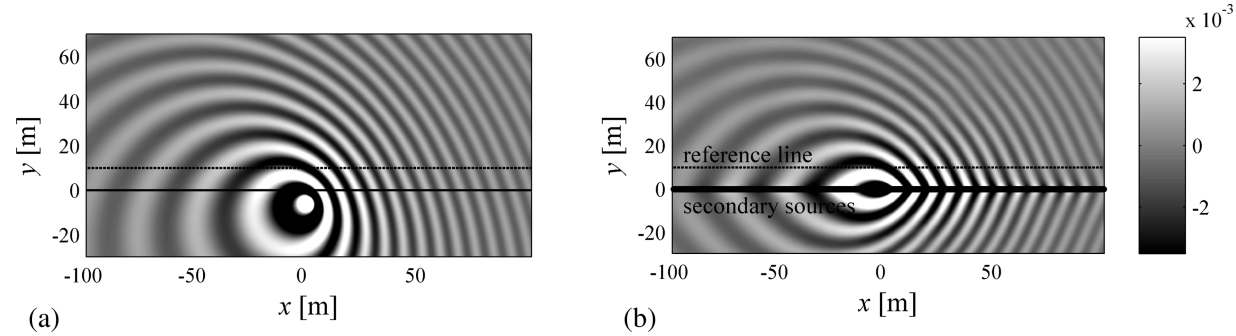

Fig. 6 The field of a monopole source moving at $\varphi = 30^\circ$ at $t = 0$ (a) calculated from the reference solution 12 and (b) synthesized by 2.5D WFS.

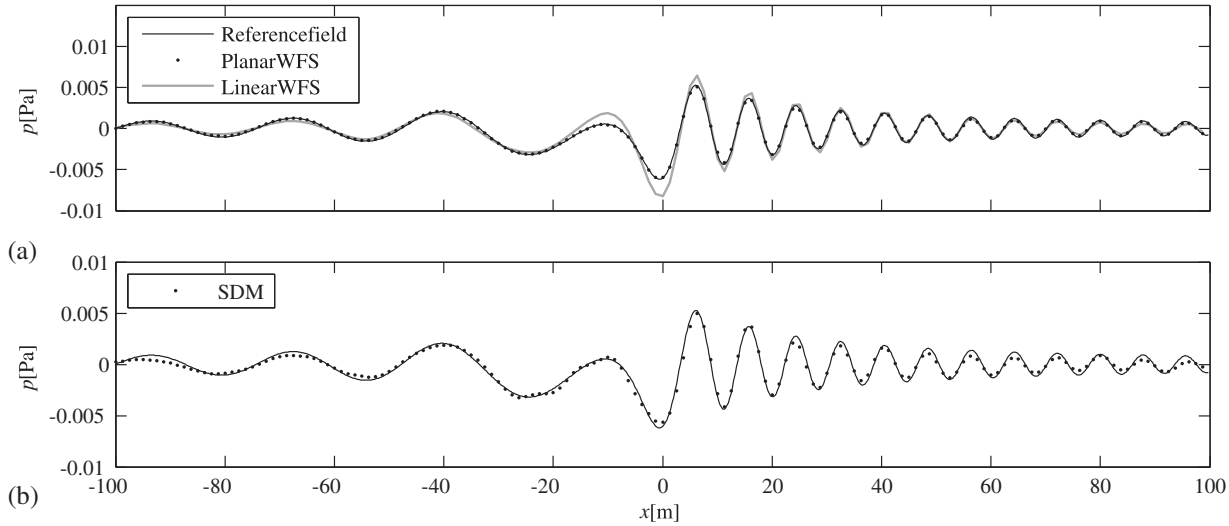

Fig. 7 The reproduction of a sound source, moving at $\varphi = 30^\circ$ to the x-axis at $t = 0$: cross-section of the synthesized sound field along the reference line using (a) WFS with planar and linear SSD, (b) and SDM.

a compact analytical formula was found for the WFS of moving sources with linear SSD. Based on the introduced wavenumber representation, explicit wavenumber domain driving functions were given for the SDM. As the main finding of the research a mathematically consistent solution was given for SFS utilizing both WFS and the SDM. For the case of a sound source moving parallel to the SSD, the frequency domain SDM driving functions were found analytically, and it was shown that similarly to the stationary case, WFS provides the far-field approximation for the reference SDM solution. Theoretically, the presented techniques are capable of handling sources with arbitrary excitation time histories. However, their direct numerical application is computationally expensive and needs further development.

6 REFERENCES

[1] E. W. Start, *"Direct Sound Enhancement by Wave Field Synthesis*," *Ph.D. thesis*, Delft Univ. of Technol., Delft, The Netherlands (1997).

[2] S. Spors, R. Rabenstein, and J. Ahrens, "The Theory of Wave Field Synthesis Revisited," presented at the *124th Convention of the Audio Engineering Society* (2008 May), convention paper 7358.

[3] E. Verheijen, "*Sound Reproduction by Wave Field Synthesis*," *Ph.D. thesis*, Delft Univ. of Technol., Delft, The Netherlands (1997).

[4] M. A. Gerzon, "Periphony: With-Height Sound Reproduction," *J. Audio Eng. Soc.*, vol. 21, pp. 2–10 (1973 Jan./Feb.).

[5] J. Ahrens and S. Spors, "An Analytical Approach to Sound Field Reproduction Using Circular and Spherical Loudspeaker Distributions," *Acta Acust. united Ac.*, vol. 94, no. 6, pp. 988–999 (2008 Nov./Dec.).

[6] J. Ahrens, *Analytic Methods of Sound Field Synthesis*, 1st edition (Springer, Berlin, 2012).

[7] F. M. Fazi and P. A. Nelson, "Sound Field Reproduction as an Equivalent Acoustical Scattering Problem," *J. Acoust. Soc. Am.*, vol. 134, no. 5, pp. 3721–3729 (2013 Nov.).

[8] J. Ahrens and S. Spors, "Sound Field Reproduction Using Planar and Linear Arrays of Loudspeakers," *IEEE Trans. Audio, Speech, Lang. Process.*, vol. 18, no. 8, pp. 2038–2050 (2010 Nov.).

[9] A. Franck, A. Graefe, K. Thomas, and M. Strauss, "Reproduction of Moving Sound Sources by Wave Field Synthesis: An Analysis of Artifacts," *Proc. of the 32nd Intl. Conf. Audio Eng. Soc.: DSP For Loudspeakers* (Sept. 2007).

[10] J. Ahrens and S. Spors, "Reproduction of Moving Virtual Sound Sources with Special Attention to the Doppler Effect," presented at the *124th Convention of the Audio Engineering Society* (2008 May), convention paper 7363.

[11] E. G. Williams, *Fourier Acoustics: Sound Radiation and Nearfield Acoustical Holography*, 1st edition (Academic Press, London, 1999).

[12] A. J. Berkhout, D. de Vries, and P. Vogel, "Acoustic Control by Wave Field Synthesis," *J. Acoust. Soc. Am.*, vol. 93, no. 5, pp. 2764–2778 (1993 May).

[13] S. Spors and J. Ahrens, "Analysis and Improvement of Pre-Equalization in 2.5-Dimensional Wave Field Synthesis," presented at the *128th Convention of the Audio Engineering Society* (2010 May), convention paper 8121.

[14] F. Schultz and S. Spors, "Comparing Approaches to the Spherical and Planar Single Layer Potentials for Interior Sound Field Synthesis," *Acta Acust. united Ac.*, vol. 100, no. 5, pp. 900–911 (2014 Sept./Oct.).

[15] P. M. Morse and K. U. Ingard, *Theoretical Acoustics*, 1st edition (McGraw-Hill Book Company, New York, NY, 1968).

[16] NIST Digital Library of Mathematical Functions, http://dlmf.nist.gov/, Release 1.0.9 of 2014-08-29.

[17] I. S. Gradshteyn and I. M. Ryzhik, *Table of Integrals, Series, and Products*, 7th edition (Academic Press, 2007).

APPENDIX

.1 DEFINITIONS OF FOURIER TRANSFORMS

The temporal Fourier transform (or frequency content) of a function $f(t)$ and the spatial Fourier transform (or wavenumber content) are defined in the same manner as in the related literature, e.g., [8]:

$$\mathcal{F}_t\{f(t)\} = F(\boldsymbol{\omega}) = \int_{-\infty}^{\infty} f(t)\,\mathrm{e}^{-\mathrm{j}\boldsymbol{\omega}t}\,\mathrm{d}t, \tag{24}$$

$$\mathcal{F}_x\{f(x)\} = \tilde{f}(k_x) = \int_{-\infty}^{\infty} f(x)\,\mathrm{e}^{\mathrm{j}k_x x}\,\mathrm{d}x \tag{25}$$

.2 SPATIAL FOURIER TRANSFORM OF THE FIELD OF A MOVING SOURCE

By using Eq. (11) and the convolution theorem [11], the Fourier transform to be evaluated is written as

$$-\frac{\mathrm{j}}{4v}\,\mathcal{F}_x\left\{H_0^{(2)}(-\mathrm{j}\hat{k}_t\,|y'|)\,\mathrm{e}^{-\mathrm{j}\hat{k}x'}\right\} = -\frac{\mathrm{j}}{4v}\,\mathcal{F}_x\left\{H_0^{(2)}(-\mathrm{j}\hat{k}_t\,|y'|)\right\} *_{k_x} \mathcal{F}_x\left\{\mathrm{e}^{-\mathrm{j}\hat{k}x'}\right\}. \tag{26}$$

The second term is the Fourier transform of an exponential and can be easily evaluated. By substituting the original coordinates, the result is written as

$$\mathcal{F}_x\left\{\mathrm{e}^{-\mathrm{j}\hat{k}x'}\right\} = 2\pi\delta(k_x - \cos\varphi\,\hat{k})\mathrm{e}^{-\mathrm{j}\hat{k}(\sin\varphi(y-y_s)-\cos\varphi x_s)}. \tag{27}$$

For the first term we utilize that the function to be transformed is even and make use of the expression [17, (6.677,9.)], with substituting $\beta = 0$

$$\mathcal{F}_x\left\{H_0^{(2)}(-\mathrm{j}\hat{k}_t\,|x|)\right\} = \frac{2\mathrm{j}}{\sqrt{k_x^2 + \hat{k}_t^2}}. \tag{28}$$

As $y' = -\sin\varphi\,x + (\sin\varphi\,x_s + \cos\varphi\,(y - y_s))$, we may use the similarity and shifting theorems to obtain:

$$\mathcal{F}_x\left\{H_0^{(2)}(-\mathrm{j}\hat{k}_t\,|x|)\right\} = \frac{2\mathrm{j}}{|\sin\varphi|}\frac{\mathrm{e}^{\mathrm{j}\frac{k_x}{\sin\varphi}(\sin\varphi\,x_s+\cos\varphi\,(y-y_s))}}{\sqrt{(-\frac{k_x}{\sin\varphi})^2 + \hat{k}_t^2}}. \tag{29}$$

The convolution will sift out $k_x = k_x - \cos\varphi\,\hat{k}$:

$$-\frac{\mathrm{j}}{4v}\mathcal{F}_x\left\{H_0^{(2)}(-\mathrm{j}\hat{k}_t\,|y'|)\,\mathrm{e}^{-\mathrm{j}\hat{k}x'}\right\} = \frac{\pi}{v|\sin\varphi|}\frac{\mathrm{e}^{-\mathrm{j}\frac{\cos\varphi\hat{k}-k_x}{\sin\varphi}(\sin\varphi x_s+\cos\varphi(y-y_s))}}{\sqrt{\left(\frac{\cos\varphi\hat{k}-k_x}{\sin\varphi}\right)^2 + \hat{k}_t^2}}\mathrm{e}^{-\mathrm{j}\hat{k}(\sin\varphi(y-y_s)-\cos\varphi x_s)}. \tag{30}$$

After rearrangement and using basic trigonometric identities, the equation takes the form as given in the body text Eq. (13).

THE AUTHORS

Gergely Firtha

Peter Fiala

Gergely Firtha was born in Budapest, Hungary, in 1986. He received his B.S. and M.S degrees from Budapest University of Technology and Economics in 2009 and 2011 respectively. Currently he is a Ph.D. student in the Laboratory of Acoustics and Studio Technology at the Department of Networked Systems and Services. His main research interests include acoustic signal processing and multichannel sound field reproduction.

Peter Fiala was born in Budapest, Hungary, in 1978. He received the Ph.D. degree in electrical engineering in 2009 from Budapest University of Technology and Economics. He is working as assistant professor at the Department of Networked Systems and Services. His main research interests are in the field of computational acoustics, acoustic signal processing, and noise and vibration control.